05.6;13.3

Amorphization of silicon nanowires upon irradiation with argon ions

© A.V. Kononina[1], Yu.V. Balakshin[1,2], K.A. Gonchar[1], I.V. Bozhev[1,3], A.A. Shemukhin[1,2], V.S. Chernysh[1,2]

[1] Moscow State University, Moscow, Russia
[2] Skobeltsyn Institute of Nuclear Physics, Moscow State University, Moscow, Russia
[3] Quantum Technologies Centre, M. V. Lomonosov Moscow State University, Moscow, Russia
E-mail: anastasiia.kozhemyako@mail.ru

Received August 10, 2021
Revised September 27, 2021
Accepted September 28, 2021

The irradiation of silicon nanowires with Ar^+ ions with the energy of 250 keV and fluences of 10^{13} to 10^{16} cm^{-2} was carried out. The dependence of the destruction of the structure under ion irradiation on the fluence was investigated by Raman spectroscopy. It was shown that the amorphization of porous silicon occurs at higher values of displacement per atom than in thin silicon films.

Keywords: silicon nanowires, Raman spectroscopy, defect formation.

DOI: 10.21883/TPL.2022.01.52470.18989

At present, silicon−based nanostructures are intensely studied in many fields of nanoelectronics [1,2]. Among silicon nanostructures, silicon nanowires has recently begun attracting a great interest. Sensitive elements fabricated based on them may be used to detect various respiratory viruses [3], silicon nanowires are used in producing highly sensitive biosensors, photoelectric devices, energy storage and conversion devices [4,5].

The effect of ion irradiation on the silicon nanowire properties and structure is so far poorly studied. However, the efficiency of this modification technique is obvious. Paper [6] has shown that irradiation with boron ions at different beam incidence angles enables controlling conductivity of a substrate made from silicon nanowires. Paper [7] demonstrates the possibility of controlling the silicon nanowire wettability by acting upon the target with a proton beam. Using ion implantation, it is possible to create in arrays of silicon nanowires $p{-}n$-junctions based on which functional devices will be constructed [8].

In analyzing the ion irradiation influence on the structures properties, it is necessary to consider not only the implanted impurities but also radiation−induced defects. Their effect on the semiconductors characteristics is quite significant. The defect concentration defines thermal conductivity [9], electron−hole current and electrical rupture conditions [10], concentration of paramagnetic centers [11], optical emission and absorption spectra in semiconductor structures [12].

In this work, dynamics of silicon nanowire amorphization under argon ion irradiation has been studied. The obtained results have been compared with data obtained on amorphization of porous and solid silicon.

The array of silicon nanowires (SNWs) was irradiated with 250 keV Ar^+ ions at fluences ranging from 10^{13} to 10^{16} cm^{-2}. The process of defect formation was studied by Raman spectroscopy (RS).

SNWs were obtained by metal−stimulated chemical etching (the EE method) of $p{-}type$ c-Si plates with the (100) crystallographic orientation and resistivity of 10−20 $\Omega \cdot$ cm. As the metal catalyst, gold was used which was removed with the „aqua regia“ solution (HCl:HNO_3).

Structural properties were studied by using scanning electron microscope (SEM) Carl Zeiss SUPRA 40 FE-SEM. SEM images of the obtained SNWs is presented in Fig. 1. As the figure shows, the SNW layer thickness was 4.5 μm, nanowire diameter was 10−50 nm, and the distance between nanowires was 100−200 nm. Nanostructures obtained by etching consist of a crystalline skeleton coated with an oxide layer. This was confirmed in a number of investigations [13,14].

Irradiation was performed at the accelerator facility HVEE-500 [15]. The experimental process line comprised an ion beam focusing system and target scanning system, as well as a neutral particle trap and a system for suppressing secondary electrons to control the radiation fluence. Irradiation was performed at room temperature, operating pressure in the chamber did not exceed 10^{-5} Pa,

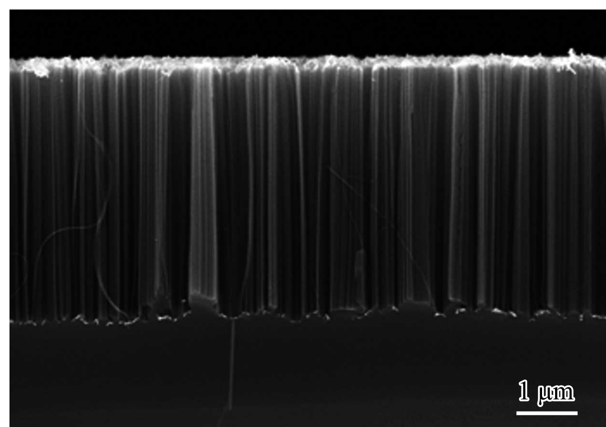

Figure 1. FEM image of the lateral cross−section of an SNW sample obtained by the MSCE method.

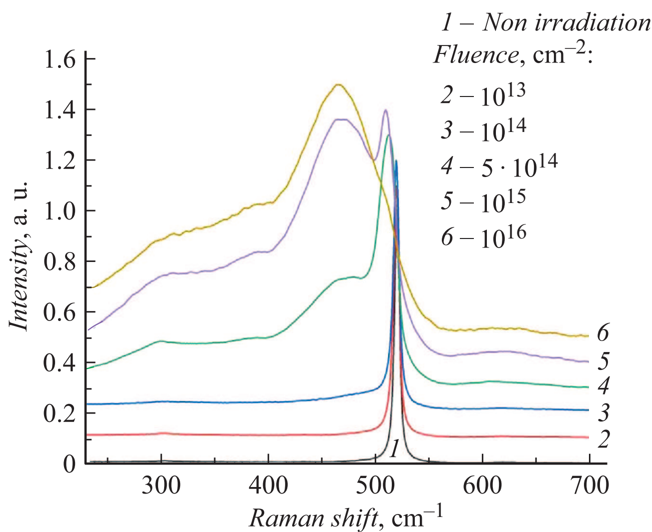

Figure 2. Intensities of the Raman spectra measured on the array of silicon nanowires prior to and after irradiation with Ar^+ ions 250 keV in energy.

the beam current density was as low as 0.5 μA/cm^2 which excluded the sample heating during irradiation.

Raman spectra were obtained at room temperature at the setup „Probing Nanolaboratory INTEGRASpectra" using a 472.9 nm laser; during measurements, the laser power was 4.2 mW/cm^2.

Fig. 2 presents the Raman spectra measured on the array of silicon nanowires prior to and after irradiation with Ar^+ ions 250 keV in energy. The Raman spectra of a non-irradiated sample and samples irradiated with low fluences contain intense peaks at 520 cm^{-1} related to the silicon crystalline phase [16]. Raman spectra of samples irradiated at higher ion fluences contain broad peaks with maxima at about 460–480 cm^{-1} and also less intense peaks at 300 and 380 cm^{-1}. The last two peaks relate to amorphous silicon [17]. The broad peak located at about 460–480 cm^{-1} may be a superposition of several peaks related to amorphous silicon (470–480 cm^{-1}) [17,18] and amorphous silicon dioxide (446 and 492 cm^{-1}) [19]. Intensity of the peak related to the crystalline phase decreases with increasing ion fluence. The peak related to the phases of amorphous silicon and silicon dioxide manifests itself first as a shoulder of the intense peak at 520 cm^{-1}; as the fluence increases, the total intensity of this group of peaks increases. This indicates the crystal structure disordering under the ion beam action. The spectrum measured on the sample irradiated with the maximal fluence is absolutely free of the peak at 520 cm^{-1} and consists of a broad peak with the maximum at about 460–480 cm^{-1}, which evidences complete amorphization of the structure.

To compare the results obtained for SNWs with data on other silicon structures, the implantation parameters were converted into universal units dpa [20] (see the table). Taking into account specific features of the nanowire

Fluence in ion/cm^2 and dpa

Fluence	
ion/cm^2	dpa
10^{16}	18
10^{15}	1.8
$5 \cdot 10^{14}$	0.9
10^{14}	0.18
10^{13}	0.02

array structure and experiment geometry, parameter dpa (displacements per atom) was calculated according to the algorithm corresponding to bulk silicon [21].

Notice that at two minimal fluences (0.02 and 0.18 dpa) the maximum of the peak related to the silicon crystalline phase retains its position at 520 cm^{-1}. When fluence is $5 \cdot 10^{14}$ cm^{-2} (0.9 dpa), this peak is shifted towards lower wave numbers by $\Delta\omega = 8$ cm^{-1}, and its maximum gets location at 512 cm^{-1}. Further increase in the fluence is followed with further increase in displacement $\Delta\omega$; when fluence is 10^{15} cm^{-2}, the maximum of this peak is located at 509 cm^{-1}, which corresponds to displacement of $\Delta\omega = 11$ cm^{-1} (Fig. 3).

Possibly, the displacement of the peak related to the signal from the silicon crystalline phase indicates manifestation of the quantum-scale effect, for instance, onset of spatial restriction of phonons in nanostructured materials because of the presence of nanoparticles less than 10 nm in size, while the displacement increase with increasing radiation fluence can evidence a decrease in the size of these particles [22,23]. The obtained results comply with those of [21] where a model has been considered which implies accumulation of simplest defects in the silicon crystal at fluences below 0.5 dpa, after which coalescence of destructed regions takes place. As the fluence increases, this results in formation of defect-free crystal clusters surrounded by amorphous silicon.

At the fluence of 1.8 dpa, the spectrum contains, along with the peak related to the amorphous phase, a pronounced peak related to the crystalline phase. However, this peak is almost absolutely absent in the monocrystal silicon films at

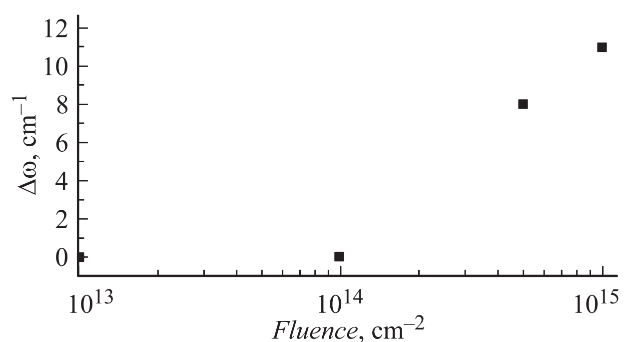

Figure 3. Displacement of the Raman peak related to the silicon crystalline phase versus the ion fluence.

the almost the same fluence of 1.7 dpa [22]. Therewith, this Raman spectrum measured on porous silicon with porosity of 50% irradiated at 2 dpa exhibits also a peak at $520\,cm^{-1}$ [11]. As Fig. 2 shows, Raman spectroscopy makes evident total destruction of the crystal structure at 18 dpa.

In conclusion, notice that Raman spectroscopy demonstrates the nanowire structure destruction at higher dpa parameters than in the case of thin silicon films. At the same time, nanowires and porous silicon (with porosity of 50%) get amorphized at dpa values close to each other.

Acknowledgements

The study was carried out by using facilities of Lomonosov Moscow State University Training Center for Lithography and Microscopy.

Financial support

The study was supported by the Russian Fundamental Research Foundation (project № 19-32-90174).

Conflict of interests

The authors declare that they have no conflict of interests.

References

[1] R. Smerdov, Yu. Spivak, I. Bizyaev, P. Somov, V. Gerasimov, A. Mustafaev, V. Moshnikov, Electronics, **10** (1), 42 (2021). DOI: 10.3390/electronics10010042

[2] R. Castro, Y. Spivak, S. Shevchenko, V. Moshnikov, Materials, **14** (10), 2471 (2021). DOI: 10.3390/ma14102471

[3] M.B. Gongalsky, U.A. Tsurikova, J.V. Samsonova, G.Z. Gvindzhiliiia, K.A. Gonchar, N.Yu. Saushkin, A.A. Kudryavtsev, E.A. Kropotkina, A.S. Gambaryan, L.A. Osminkina, Results Mater. **6**, 100084 (2020). DOI: 10.1016/j.rinma.2020.100084

[4] N. Chartuprayoon, M. Zhang, W. Bosze, Y.-H. Choa, N.V. Myung, Biosens. Bioelectron., **63**, 432 (2015). DOI: 10.1016/j.bios.2014.07.043

[5] A.V. Pavlikov, O.V. Rakhimova, P.K. Kashkarov, Moscow Univ. Phys. Bull., **73** (2), 199 (2018). DOI: 10.3103/S0027134918020121.

[6] S. Aziza, A. Ripp, D. Horvitz, Y. Rosenwaks, Mater. Sci. Semicond. Process., **75**, 43 (2018). DOI: 10.1016/j.mssp.2017.11.001

[7] V.S. Vendamani, D. Kanjilal, S. Venugopal Rao, Chem. Phys., **548**, 111242 (2021). DOI: 10.1016/j.chemphys.2021.111242

[8] S. Hoffmann, J. Bauer, C. Ronning, Th. Stelzner, J. Michler, C. Ballif, V. Sivakov, S.H. Christiansen, Nano Lett, **9** (4), 1341 (2009). DOI: 10.1021/nl802977m

[9] M.G. Shahraki, Z. Zeinali, J. Phys. Chem. Solids, **85**, 233 (2015). DOI: 10.1016/j.jpcs.2015.06.001

[10] A.A. Shemukhin, Yu.V. Balakshin, V.S. Chernysh, A.S. Patrakeev, S.A. Golubkov, N.N. Egorov, A.I. Sidorov, B.A. Malyukov, V.N. Statsenko, V.D. Chumak, Tech. Phys. Lett., **38** (10), 907 (2012). DOI: 10.1134/S1063785012100112.

[11] A.P. Evseev, A.V. Kozhemiako, Yu.V. Kargina, Yu.V. Balakshin, E.A. Zvereva, V.S. Chernysh, M.B. Gongalsky, A.A. Shemukhin, Rad. Phys. Chem., **176**, 109061 (2020). DOI: 10.1016/j.radphyschem.2020.109061

[12] S.D. Trofimov, S.A. Tarelkin, S.V. Bolshedvorskii, V.S. Bormashov, S.Yu. Troshchiev, A.V. Golovanov, N.V. Luparev, D.D. Prikhodko, K.N. Boldyrev, S.A. Terentiev, A.V. Akimov, N.I. Kargin, N.S. Kukin, A.S. Gusev, A.A. Shemukhin, Yu.V. Balakshin, S.G. Buga, V.D. Blank, Opt. Mater. Express, **10** (1), 198 (2020). DOI: 10.1364/OME.10.000198

[13] Y.M. Spivak, A.Y. Gagarina, M.O. Portnova, A.V. Zaikina, V.A. Moshnikov, J. Phys.: Conf. Ser., **1697**, 012126 (2020). DOI: 10.1088/1742-6596/1697/1/012126

[14] Yu.M. Spivak, S.V. Myakin, V.A. Moshnikov, M.F. Panov, A.O. Belorus, A.A. Bobkov, J. Nanomater., **2016**, 2629582 (2016). DOI: 10.1155/2016/2629582

[15] Yu.V. Balakshin, A.A. Shemukhin, A.V. Nazarov, A.V. Kozhemiako, V.S. Chernysh, Tech. Phys., **63** (12), 1861 (2018). DOI: 10.1134/S106378421812023X.

[16] Z. Sui, P.P. Leong, I.P. Herman, G.S. Higashi, H. Temkin, Appl. Phys. Lett., **60** (17), 2086 (1992). DOI: 10.1063/1.107097

[17] D. Bermejo, M. Cardona, J. Non-Cryst. Solids, **32** (1-3), 405 (1979). DOI: 10.1016/0022-3093(79)90085-1

[18] N.E. Maslova, A.A. Antonovsky, D.M. Zhigunov, V.Y. Timoshenko, V.N. Glebov, V.N. Seminogov, Semiconductors, **44** (8), 1040 (2010). DOI: 10.1134/S1063782610080154.

[19] R.K. Biswas, P. Khan, S. Mukherjee, A.K. Mukhopadhyay, J. Ghosh, K. Muraleedharan, J. Non-Cryst. Solids, **488**, 1 (2018). DOI: 10.1016/j.jnoncrysol.2018.02.037

[20] K.V. Karabeshkin, P.A. Karaseov, A.I. Titov, Semiconductors, **47** (2), 242 (2013). DOI: 10.1134/S1063782613020115.

[21] Yu.V. Balakshin, A.V. Kozhemiako, A.P. Evseev, D.K. Minnebaev, E.M. Elsehly, Moscow Univ. Phys. Bull., **75** (3), 218 (2020). DOI: 10.3103/S0027134920030030.

[22] A.V. Kozhemiako, A.P. Evseev, Yu.V. Balakshin, A.A. Shemukhin, Semiconductors, **53** (6), 800 (2019). DOI: 10.1134/S1063782619060095.

[23] A. Colli, A. Fasoli, C. Ronning, S. Pisana, S. Piscanec, A.C. Ferrari, Nano Lett., **8** (8), 2188 (2008). DOI: 10.1021/nl080610d